Supplementary Materials

S1. Table of the Camera performance parameter

Table S1. Camera performance parameter table

Parameter list	Parameter
Brands	OptiTrack
Model	Prime17
Structure size	126×126×110mm
Resolution	1688×1064
Frame rate	360
Lens	6mm
Aperture	F#1.6
CCD chip	2/3 inch（height6.6mm; width8.8mm）
Subtlety of IR	at 850nm IR
Subtlety of LEDs	20 ultra high power LEDs
Angle range	Horizontal viewing angle 70°, Vertical viewing angle 49°

S2. Calculation of the definition domain of the corresponding parameters of different layouts

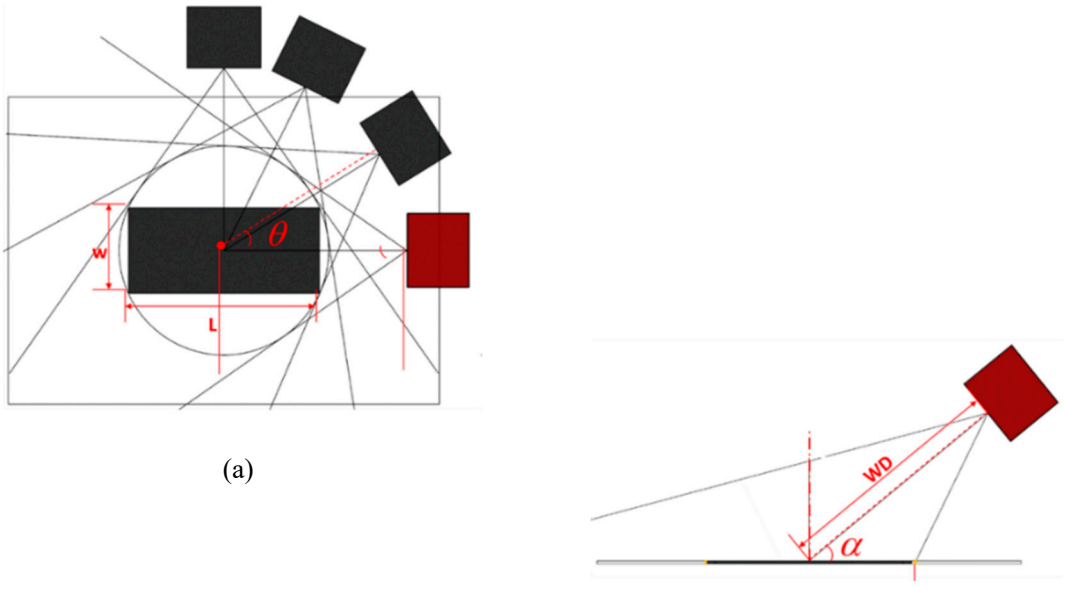

(a) (b)

Figure S1. Schematic layout of a multi-camera simplified view (**a**) Top view; (**b**) Side view

The working field of view (length *L* and width *W*) [1, 2]is determined by the lens-to-shot object or the distance to target moving plane (*WD*), focal length (*f*), and chip size (height *h*, width *v*), and the relationship is determined by the Eq. S-1:

$$L = WD \times (h/f)\ ; \quad W = WD \times (v/f) \tag{S-1}$$

The premise for motion capture is that the area where the object is captured is within the intersecting field of view of multiple cameras, in order to compare the intersecting volumes of the three layout forms. First of all, it is necessary to define the domain of layout parameters corresponding to different layout forms, and the relationships to be satisfied between the

parameters. Through the calculation of the theoretical model, the following relationship is obtained:

① When a four-camera system takes the arched layout, if $f \in [6, 7.95)$, then $\alpha \in (0^\circ, 90^\circ]$, and if $f \in [7.95, 9.6]$, then $\alpha \in (21.55^\circ, 90^\circ]$.

② When a four-camera system adopts the annular or a half-annular layout, it must be satisfied that $f \in [6, 7.95)$, then $\alpha \in (16.6^\circ, 43.7^\circ]$, and if $f \in [7.95, 9.6]$, then $\alpha \in (43.7^\circ, 53.2^\circ]$.

S3. The relationship between layout parameters corresponding to different camera layout

①Arch layout - the relationship between focal length *f* and pitch angle α

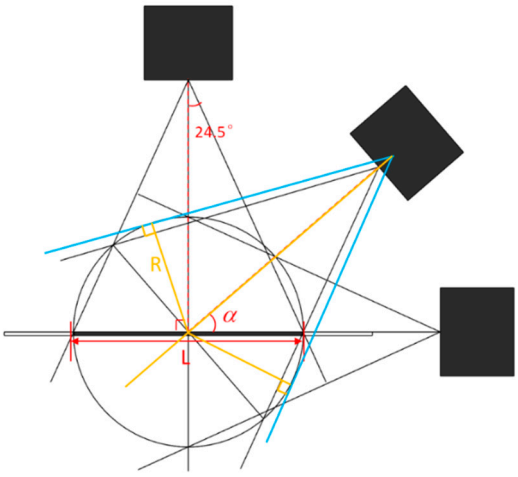

Figure S2. Simplified view of the intersection of the angle of view and the target plane of motion in the arched layout of the camera (side view)

As we know that, $H = 6.6$, if $f \in [6, 9.6]$, there are the following equation:

$$\begin{cases} WD = f \cdot L / H \\ R \geq L/2 \\ R = WD \cdot \sin 24.5^\circ \end{cases} \tag{S-2}$$

The formula S-1 was brought to the Eq. S-3, and then solved it, thus we had the solution $f \geq 7.95$, when if $7.95 \leq f \leq 9.6$, because $\alpha \in (0^\circ, 90^\circ]$, when $6 \leq f \leq 7.95$, the following equation:

$$\begin{cases} WD = (f \cdot L)/H \\ WD \cdot \cos\alpha - WD \cdot \sin\alpha / \tan(\alpha + 24.5^\circ) \geq L/2 \end{cases} \tag{S-3}$$

The above equation was simplified and the following equation was gained:

$$\cos\alpha - \sin\alpha / \tan(\alpha + 24.5^\circ) = \frac{3.3}{f} \tag{S-4}$$

And then $M = \cos\alpha - \sin\alpha / \tan(\alpha + 24.5^\circ)$ was defined, as $6 \leq f \leq 7.95$, the definition of pitch angle α was $21.55^\circ \leq \alpha \leq 65.92^\circ$.

②Half-annular layout - the relationship between focal length *f* and pitch angle α

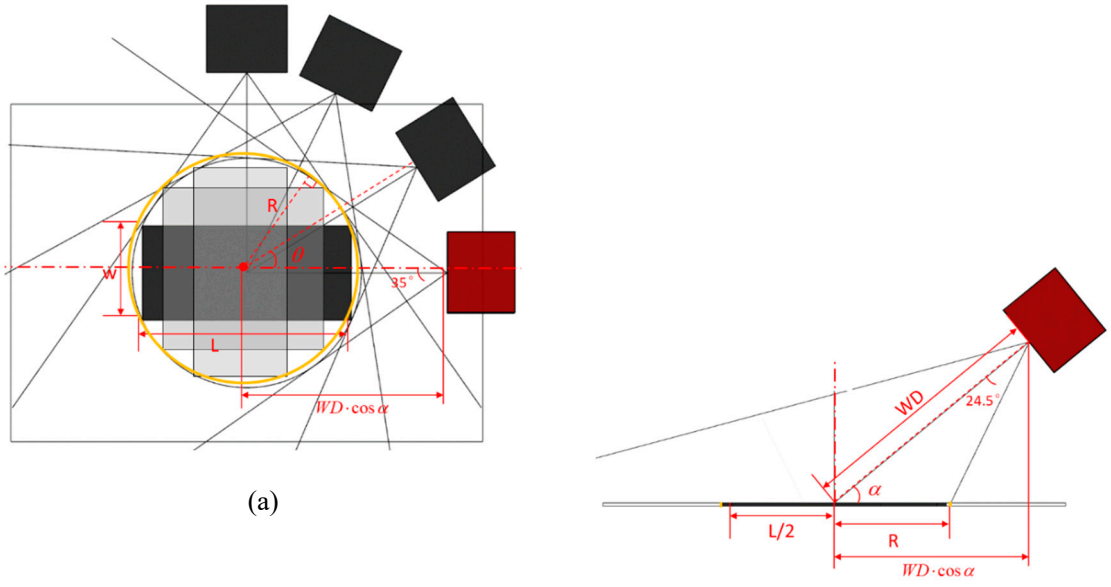

(a) (b)

Figure S3. Simplified view of the intersection of the view angle range with the target motion plane in the annular layout of the camera (**a**) Top view; (**b**) Side view

It could be seen from Figure **S3 t**hat When $WD \cdot \cos\alpha \cdot \sin\beta \geq R$, there was the following equation:

$$\begin{cases} R = (\sqrt{L^2 + w^2})/2 \\ WD \cdot \cos\alpha \cdot \sin 35^\circ \geq R \\ WD = (f \cdot L)/H \end{cases} \quad \text{(S-5)}$$

If $f \in [7.95, 9.6]$ and $\alpha \in (0^\circ, 90^\circ)$, because $\cos\alpha > 5.75/f$, so $\alpha_{\min} = 43.7^\circ$ and $\alpha_{\max} = 53.2^\circ$; If $f \in [6, 7.95]$ and $\alpha \in [21.55^\circ, 65.92^\circ]$, because $\alpha \geq 21.55^\circ$, at this time, $\cos\alpha \approx 0.93 = 5.75/f$, so $f = 6.2$, meanwhile, the angle θ between the cameras could take any value $\theta \in (0, 90^\circ)$.

S4. The intersecting volume of the multi-camera system a unit module

1) Arched layout. The intersecting volume of multi-camera's unit module approximated half of the cylinder:

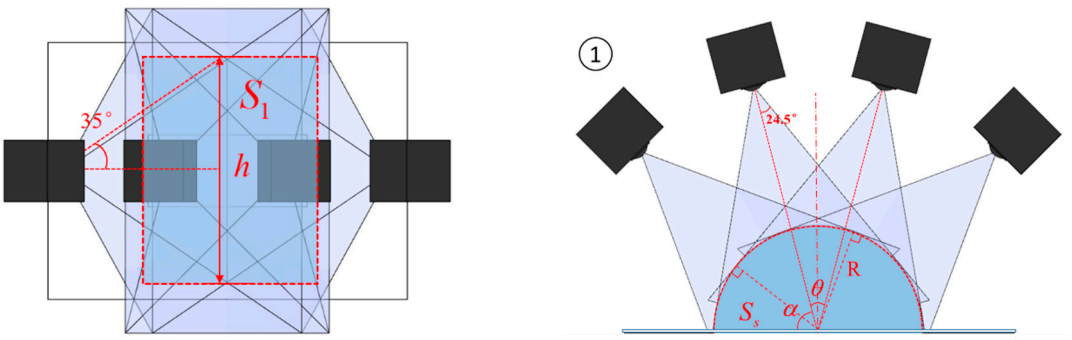

(a) (b)

Figure S4. Simplified schematic view of the intersecting volume of a multi-camera unit module in the arch layout (**a**) Top view; (**b**) Side view

$$\begin{cases} V_1 = S_s \cdot h \\ S_s = 0.5 \cdot \pi \cdot R^2 \\ S_1 = 2 \cdot R \cdot h \end{cases} \tag{S-6}$$

$$\begin{cases} R = WD \cdot \sin 24.5^\circ \\ h = 2 \cdot WD \cdot \cos\alpha \cdot \tan 35^\circ \end{cases} \tag{S-7}$$

Through Eq. S-1, Eq. S-6 and Eq. S-7:

$$\begin{cases} S_s = 0.27 \cdot WD^2 \\ S_1 = 0.581 \cdot WD^2 \\ V_1 = 0.378 \cdot \cos\alpha \cdot WD^3 \end{cases} \tag{S-8}$$

The intersecting volume of the field of view in this layout could be abstracted by the inner enveloping cuboid (length L_1, width W_1, height H_1):

$$L_1 = h; W_1 = 2 \cdot R; H_1 = R \tag{S-9}$$

Equation S-8 was brought to S-9 to get the following equation:

$$L_1 = 1.4 \cdot WD; W_1 = 0.83 \cdot WD; H_1 = 0.415 \cdot WD \tag{S-10}$$

According to Eq. S-10, we got the Eq. S-11:

$$W_1 = 0.593 \times L_1; H_1 = 0.296 \times L_1 \tag{S-11}$$

2) Half-annular layout, the angle between the cameras (θ) was assumed to be equal, and the intersecting volume is approximately a combination of a half circle body and a triangular table, as shown in Figure S5.

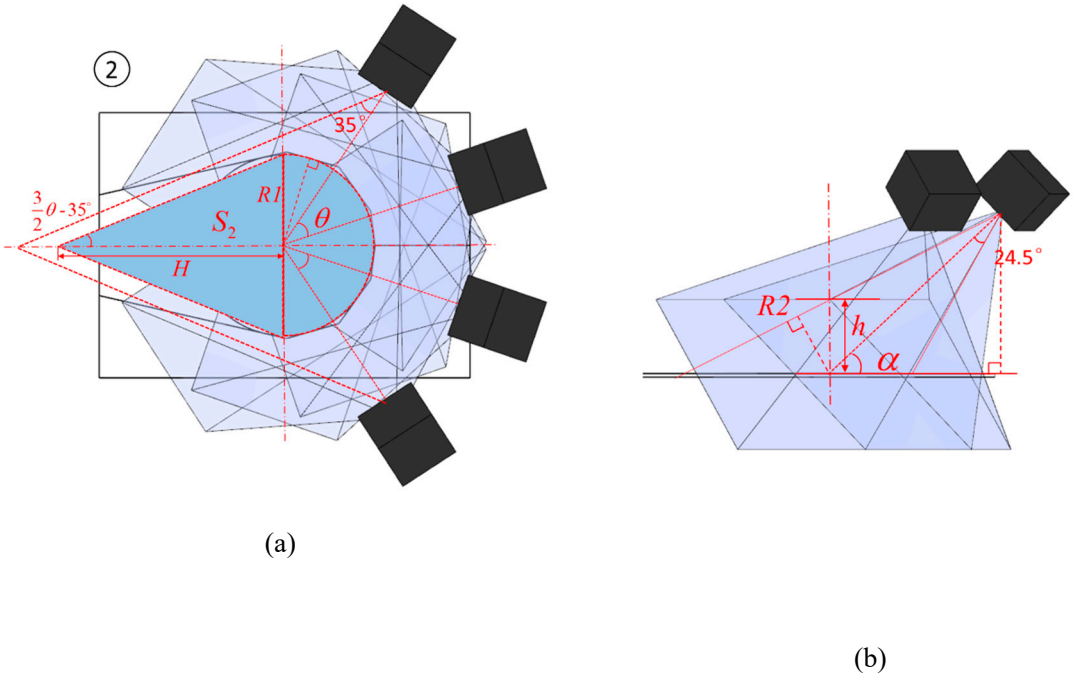

Figure S5. Simplified schematic view of the intersecting volume of a multi-camera unit module in the half-annular layout (**a**) Top view; (**b**) Side view

$$\begin{cases} V_2 = S_2 \cdot h \\ S_2 = S_a + S_b \\ S_a = 0.5 \cdot \pi \cdot R_1^2 \\ S_b = 2 \cdot R_1 \cdot H \cdot 0.5 \end{cases} \quad (S\text{-}12)$$

$$R_1 = WD \cdot \cos\alpha \cdot \sin 35^\circ; R_2 = WD \cdot \sin 24.5^\circ \quad (S\text{-}13)$$

$$h = R_2 / \cos(\alpha - 24.5^\circ); H = R_1 / \tan(1.5\theta - 35^\circ) \quad (S\text{-}14)$$

Eq. S-1, Eq. S-13 and Eq. S-14 were combined, and the result was obtained as following equation:

$$\begin{cases} h = 0.415 \cdot WD / \cos(\alpha - 24.5^\circ) \\ H = 0.574 \cdot WD \cdot \cos\alpha / \tan(1.5\theta - 35^\circ) \end{cases} \quad (S\text{-}15)$$

Eq. S-12 and Eq. S-15 were combined, and the result was obtained as following equation:

$$\begin{cases} S_2 = (0.517 + \dfrac{0.238}{\tan(1.5\theta - 35^\circ)}) \cdot \cos\alpha^2 \cdot WD^2 \\ V_2 = (0.215 + \dfrac{0.099}{\tan(1.5\theta - 35^\circ)}) \cdot \dfrac{\cos\alpha^2}{\cos(\alpha - 24.5^\circ)} \cdot WD^3 \end{cases} \quad (S\text{-}16)$$

The intersecting volume of the field of view in this layout can be abstracted by the inner enveloping cuboid (length L_2, width W_2, height H_2):

$$L_2 = H + R_1; W_2 = 2 \cdot R_1; H_2 = h \quad (S\text{-}17)$$

Equation S-1 and equation S-14 are brought into the equation S-16, and the equation S-18 was gained:

$$\begin{cases} L_2 = 0.573WD \cdot \cos\alpha / (\tan(1.5\theta - 35^\circ) + 1) \\ W_2 = 1.147 \cdot WD \cdot \cos\alpha \\ H_2 = 0.415 \cdot WD / \cos(\alpha - 24.5^\circ) \end{cases} \quad (S\text{-}18)$$

The equation for calculating the size ratio of the inner cuboid of the intersecting volume under the layout was as follows: P_1 was the ratio of width to length, and P_2 was the ratio of height to length.

$$\begin{cases} P_1 = \dfrac{W_2}{L_2} = 2(tan(1.5\theta - 35^o) + 1) \\ P_2 = \dfrac{H_2}{L_2} = \dfrac{0.724(tan(1.5\theta - 35^o) + 1)}{cos(\alpha - 24.5^o)} \end{cases} \quad (S\text{-}19)$$

There α and θ were ensured within the definition range. When $\theta \in (23.5^\circ, 60^\circ)$ and $\alpha \in (16.7^\circ, 53.2^\circ)$, then $P_1 \in (2.01, 4.79)$, $P_2 \in (0.727, 1.97)$, On the contrary, the range of width W_2 and height H_2 with respect to length L_2 obtained by Eq. S-18:

$$W_2 = (2.01, 4.79) \cdot L_2; H_2 = (0.727, 1.97) \cdot L_2 \quad (S\text{-}20)$$

3) Annular layout. The intersecting volume was approximately square, then:

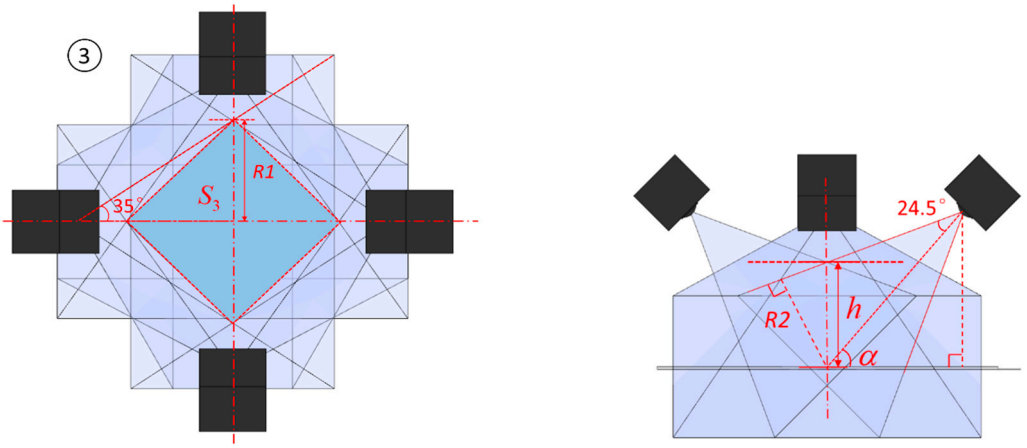

(a) (b)

Figure S6. Simplified schematic view of the intersecting volume of a multi-camera unit module in the annular layout (**a**) Top view; (**b**) Side view

$$\begin{cases} V_3 = S_3 \cdot h \\ S_3 = 0.5 \cdot (WD \cdot \cos\alpha \cdot \tan 35^\circ)^2 \times 4 \\ R = WD \cdot \sin 24.5^\circ \\ h = R/\cos(\alpha - 24.5^\circ) \end{cases} \quad \text{(S-21)}$$

Solved by Eq. S-21:

$$S_3 = 0.98 \cdot \cos\alpha^2 \cdot WD^2; V_3 = 0.41 \cdot \frac{\cos\alpha^2}{\cos(\alpha - 24.5^\circ)} \cdot WD^3 \quad \text{(S-22)}$$

The intersecting volume of the field of view in this layout could be abstracted by the inner enveloping cuboid (length L_3, width W_3, height H_3):

$$L_3 = W_3 = R_1; H_3 = h \quad \text{(S-23)}$$

Combined the equation S-20 and S-22:

$$L_3 = W_3 = 0.7 \cdot \cos\alpha \cdot WD; H_3 = 0.415 \cdot WD/\cos(\alpha - 24.5^\circ) \quad \text{(S-24)}$$

The equation for the ratio of the size of the inner envelope cuboid under the intersecting volume of this layout was as follows:

$$P_1 = \frac{W_3}{L_3}; P_2 = \frac{H_3}{L_3} \quad \text{(S-25)}$$

Ensured that α and θ are within the definition range. When $\theta \in (23.5^\circ, 60^\circ)$ and $\alpha \in (21.6^\circ, 90^\circ)$, combined the equation S-23 and S-24, we could got the results： $P_1 \in (2.01, 4.79)$, $P_2 \in (0.727, 1.97)$, moreover, according to the Eq. S-24, we obtained the Eq. S-25, and then the range of width W_2 and height H_2 with respect to length L_2 obtained by Eq. S-26 and Eq. S-27:

$$W_3 = P_1 \times L_3; H_3 = P_2 \times L_3 \quad \text{(S-26)}$$

$$W_3 = L_3; H_3 = (0.635, 1.114) \cdot L_3 \quad \text{(S-27)}$$

Since h was a fixed value of 6.6, L is the length of the captured field of view, defined by the existing three-dimensional force measuring platform whose length (L) was 300mm, defined as: $\tilde{V}=V/(L/H)^3$. A function relationship: $\tilde{V}=y(f^3)$ was created. Since it was a linear relationship with V, the change law of the intersecting volume V could be replaced by a change rule. A three-dimensional space map of focal length f and pitch angle α could be obtained from the equation:

$$\begin{cases} V_1 = 0.378 \cdot WD^3 = 0.378 \cdot (\dfrac{f \cdot L}{h})^3 \\ V_2 = (0.215 + \dfrac{0.099}{\tan(1.5\theta - 35^\circ)}) \cdot \dfrac{\cos\alpha^2}{\cos(\alpha - 24.5^\circ)} \cdot WD^3 \\ V_3 = (0.41 \cdot \dfrac{\cos\alpha^2}{\cos(\alpha - 24.5^\circ)}) \cdot WD^3 \end{cases} \quad \text{(S-28)}$$

$$\begin{cases} \dfrac{V_1}{(L/h)^3} = 0.378 \cdot f^3 \\ \dfrac{V_2}{(L/h)^3} = (0.215 + \dfrac{0.099}{\tan(1.5\theta - 35^\circ)}) \cdot \dfrac{\cos\alpha^2}{\cos(\alpha - 24.5^\circ)} \cdot f^3 \\ \dfrac{V_3}{(L/h)^3} = (0.41 \cdot \dfrac{\cos\alpha^2}{\cos(\alpha - 24.5^\circ)}) \cdot f^3 \end{cases} \quad \text{(S-29)}$$

The range of θ was determined as following:

$$V_2 = (0.215 + \frac{0.099}{\tan(1.5\theta - 35^\circ)}) \cdot \frac{\cos\alpha^2}{\cos(\alpha - 24.5^\circ)} \cdot WD^3 \quad \text{(S-30)}$$

Ensuring that $\tan(1.5\theta - 35^\circ) > 0$, and the result $\theta > 23.33^\circ$ was gotten, When in a half-annular layout, $3 \times \theta \le 180^\circ$, so $\theta \in (23.33^\circ, 60^\circ]$.

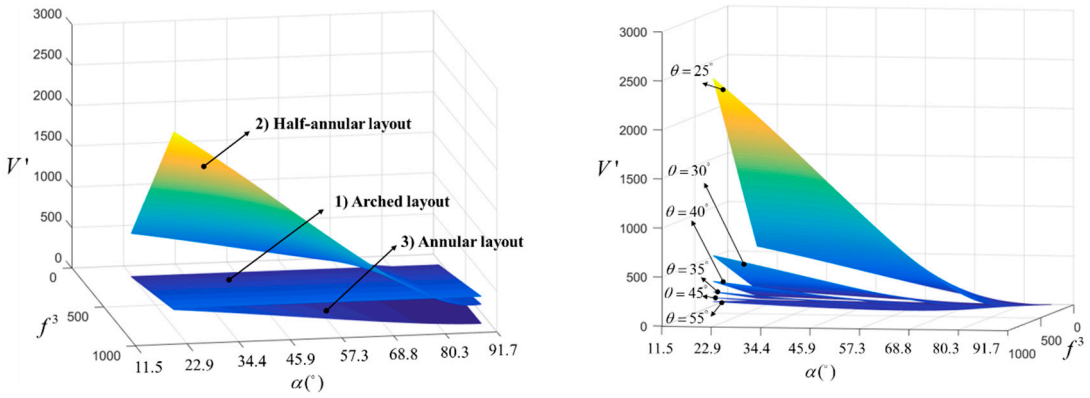

(a) (b)

Figure S7. Comparison of the intersecting volume of the three layouts of the unit module of multi-camera system (**a**) The relationship between the intersecting volume, the focal length f and the pitch angle α in the three camera configurations (θ was 25°); (**b**) The relationship between the intersecting volume, focal length f and pitching angle α when θ was different in the half-annular layout

S5. The limitation of Camera actual depth of field to the motion capture zone

The depth of field of a camera was related to the pitch angle α. The calculation of the depth of field was shown in equation S-31. The calculation of the actual depth of field ADF on the test platform can be seen in equation S-32.

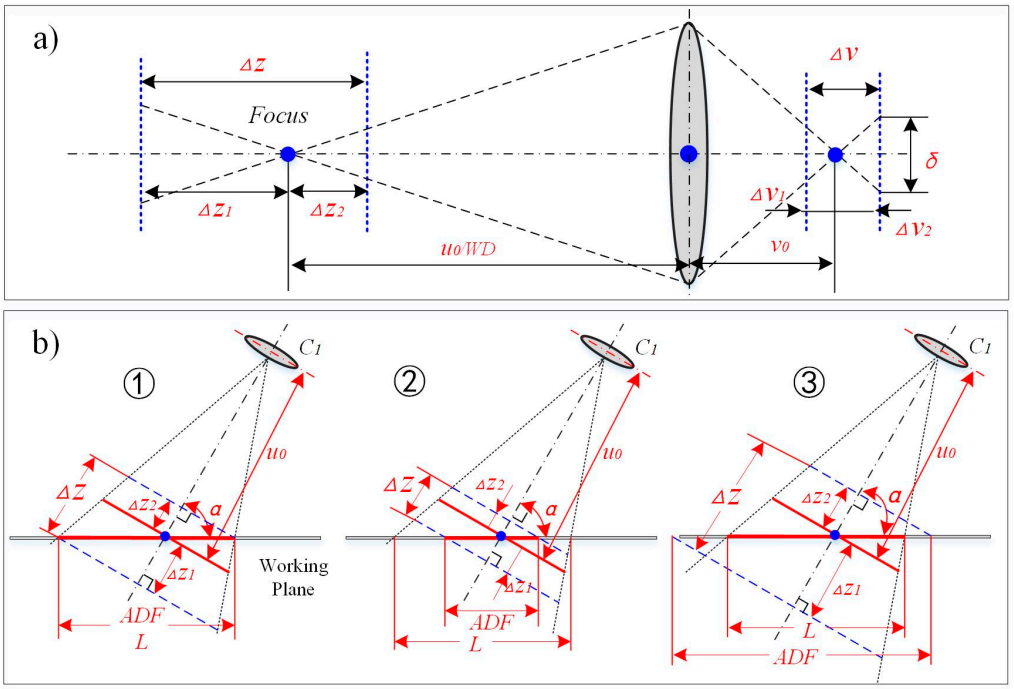

Figure S8. Relationship between camera's depth of field and length of working field

The length of working field L had a certain relationship with the actual depth of field ADF. When $L>ADF$ (FigureS8-(2)), some areas in the sampling area exceeded the depth of field, and clarity cannot be guaranteed; when $L\leq ADF$ (Figure S8-b-(1) and (3)), the sharpness could be ensured in the sampling area, and thus $L\leq ADF$ needed to be satisfied. In formula S-32, δ could be automatically calculated by the software according to the focal length, f=6, F=1.6, and then we know that $WD\in[350,700]$. From the formula S-33, we could see $L\geq 300$, since δ, f, F were fixed values. Therefore, we needed to solve the matching relationship between variables WD and α, and put S-32 into S-33. When WD was 350mm, the range of α obtained should be greater than or equal to 66.5°; when WD was greater than 540mm, α was available choosing any value within the defined domain.

$$\begin{cases} \Delta Z_1 = \dfrac{F\cdot\delta\cdot WD^2}{f^2+F\cdot\delta\cdot WD} \\ \Delta Z_2 = \dfrac{F\cdot\delta\cdot WD^2}{f^2-F\cdot\delta\cdot WD} \\ \Delta Z = \Delta Z_1+\Delta Z_2 = \dfrac{2\cdot f^2\cdot F\cdot\delta\cdot WD^2}{f^4-F^2\cdot\delta^2\cdot WD^2} \end{cases} \tag{S-31}$$

$$\begin{cases} ADF = \dfrac{\Delta Z_1}{\cos\alpha}+\dfrac{\Delta Z_2}{\cos\alpha} = \dfrac{\Delta Z}{\cos\alpha} \\ L\leq ADF \end{cases} \tag{S-32}$$

S6. Calculation of the average deviation rate

The accuracy of the motion capture process was an important indicator of the performance of the capture system. In this paper, the average capture deviation rate (*ACDR*) of a standard calibration bar in the motion capture process was used to verify the impact of the layout patterns on the accuracy of motion capture, and *ASDR* is mean value the standard deviation rates (*SDR*) of multiple experiments. The spatial coordinates of the two selected points P1 and P2 at the

moment were (X_{P1ti}, Y_{P1ti}, Z_{P1ti}), (X_{P2ti}, Y_{P2ti}, Z_{P2ti}). For the motion capture experiment of small animals, the difference CD_i, the capture deviation rate CDR_i and the *SD* of the length *Di* measured by the capture system at each moment compared to the actual measured length L_{ref}, as shown in the following Eq. S-33 to Eq. S-35, where n is the total number of frames of the selected sample video, and m is the total frame number of sample video.

$$D_i = \sqrt{(X_{P1ti} - X_{P2ti})^2 + (Y_{P1ti} - Y_{P2ti})^2 + (Z_{P1ti} - Z_{P2ti})^2} \quad \text{(S-33)}$$

$$\begin{cases} CD_i = L_{ref} - D_i \\ ACD = \sum_{i=1}^{n} (DV_i) / n \\ CDR_i = DV_i / L_{ref} \\ ACDR = \sum_{j=1}^{m} (CDR_i) / m \end{cases}, \quad \begin{matrix} (i = 1,2,\cdots,n; \\ j = 1,2,\cdots m) \end{matrix} \quad \text{(S-34)}$$

$$\begin{cases} \overline{D} = (\sum_{i=1}^{m} D_i) / n \\ SD = \sqrt{(\sum_{i=1}^{n} (D_i - \overline{D})^2) / n} \\ SDR = (SD / \overline{D}) \times 100\% \\ ASDR = (\sum_{j=1}^{m} DR_j) / m \end{cases}, \quad \begin{matrix} (i = 1,2,\cdots,n; \\ j = 1,2,\cdots m) \end{matrix} \quad \text{(S-35)}$$

S7. Motion Capture Experiment Results Statistics

Table S2. Comparison of four-camera in three typical layouts

Camera layouts	Arch	Annular	Half -annular
	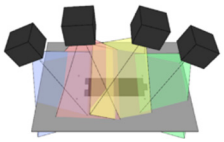	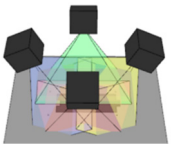	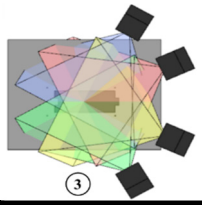
α (°)	25°,65°(45°)	45°	45°
θ (°)	30°	30°	30°
Calibrating markers' distance	43.4	43.4	43.4
WD (mm)	590±19.5	590.0±22.5	590±29.5
V(cm^3)	5.22×10^4	4.73×10^4	6.1×10^4
ACD(mm)	-0.02±0.01	20.10±5.09	-0.10±0.01
ACDR(%)	-0.05±0.02	46.31±11.73	-0.23±0.02
ASDR(%)	0.67±0.11	22.42±1.46	0.34±0.13

The measurement data, including *WD*, *ACD*, *ACDR* and *ASDR*, are presented in table S2 as mean ± standard deviation (mean ± s.d.)

Table S3. The *ASDR* at different depths of field in different multi-camera layouts

Camera layouts	*WD* (mm)	α (°)	*DF* (mm)	*ADF* (mm)	*L* (mm)	*ASDR* (%)
Arch	390	45	150	212.1	L＜212	0.84±0.07
					212<L<300	1.42±0.61

					300<L	1.59±0.25
Annular	390	45	150	212.1	L<212	6.47±5.39
					212<L<300	28.35±88.34
					300<L	50.12±68.12
Half-annular	390	45	150	212.1	L<212	0.60±0.17
					212<L<300	0.77±0.16
					300<L	1.08±0.12

The measurement data *ASDR is* presented in table S3 as mean ± standard deviation (mean ± s.d.)

Table S4. The *ASDR* at different depths of field in a half-annular layout

α(°)	θ(°)	*WD* (mm)	*DF*（mm）	*L*（mm）	*ADF*（mm）	*ASDR*（%）
30°					173.2	1.05±0.13
45°	30°	390	150	300	212.1	0.77±0.14
60°					300	0.62±0.16

The measurement data *ASDR is* presented in table S4 as mean ± standard deviation (mean ± s.d.)

Table S5. Statistical analysis of the motion capture experiment for geckos

Body parts	Measured length-L_{ref} (mm)	Mean value (mm)	Standard deviation (mm)	Mean deviation (mm)	Maximum deviation (mm)	*ACDR* (%)	*ASDR* (%)
Head	21.50±0.82	20.38	0.68	1.13	2.51	2.49	3.34
	19.50±1.05	19.47	0.49	1.03	3.74	2.04	2.52
	19.50±1.05	19.92	0.67	1.87	3.18	1.84	3.35
	20.00±0.80	19.89	0.80	1.44	2.64	2.03	4.03
Mean value						2.1±0.28	3.32±0.62
Legs	20.40±1.08	20.39	1.22	1.00	2.13	4.67	6.00
	18.50±0.48	16.93	0.88	2.01	2.55	5.30	5.23
	18.50±0.48	17.62	0.44	1.32	2.19	4.76	2.50
	21.50±2.04	20.44	0.49	1.06	2.22	4.34	2.40
Mean value				1.36±0.40		4.77±0.40	4.03±1.85
Mean value						3.43±1.46	3.67±1.33

The measurement data, including L_{ref}, *ACDR* and *ASDR*, are presented in table S5 as mean ± standard deviation (mean ± s.d.)

Table S6. Statistical analysis of the motion capture experiment for spiders

Body parts	Measured length-L_{ref} (mm)	Mean value(mm)	Standard deviation (mm)	Mean deviation (mm)	Maximum deviation (mm)	*ACDR* (%)	*ASDR* (%)
Legs	15.18±0.74	15.54	0.37	0.41	2.01	1.95	2.39
	14.8±1.36	13.93	0.62	0.84	1.66	1.68	4.45
	17.28±2.06	16.31	0.91	0.99	2.70	1.85	5.55
	17.02±1.64	16.08	0.54	1.22	2.21	1.58	3.35
	13.44±0.62	12.57	0.52	0.60	2.11	1.72	4.16

	13.67±0.56	13.26	0.44	0.37	1.39	1.79	3.30
	13.44±0.62	13.56	0.40	0.49	1.18	1.78	2.97
	13.67±0.56	13.08	0.51	0.32	2.25	1.55	3.89
Mean value				0.66± 0.33		1.74± 0.13	3.76± 0.98

The measurement data, including L_{ref}, *ACDR* and *ASDR*, are presented in table S6 as mean ± standard deviation (mean ± s.d.)

References

1. Yang, P.; Liou, K. N. Geometric-optics-integral-equation method for light scattering by nonspherical ice crystals. *Appl. Optics*. **1996**,35,6568-6584.
2. Kingslake, R.; Shannon, R. R.; Wyant, J. C. Applied optics and optical engineering. *Optica Acta International Journal of Optics*. **1969**,27,445.